Molecular Disorder and Mesoscopic Order in Polydisperse Acrylic Block Copolymers Prepared by Controlled Radical Polymerization

Anne-Valérie Ruzette,* Sylvie Tencé-Girault, and Ludwik Leibler

Laboratoire Matière Molle et Chimie (UMR 7167 ESPCI−CNRS), ESPCI, 10 rue Vauquelin, 75005 Paris, France

Florence Chauvin† and Denis Bertin

Laboratoire Chimie, Biologie et Radicaux Libres (UMR 6517), Université d'Aix-Marseille 1, 2 et 3-CNRS, Marseille, France

Olivier Guerret‡ and Pierre Gérard

Groupement de Recherche de Lacq, ARKEMA, Lacq, France

Received March 10, 2006; Revised Manuscript Received June 9, 2006

ABSTRACT: Self-assembly of high molecular weight polydisperse acrylic block copolymers and their blends is presented under conditions as close as possible to thermodynamic equilibrium. Di- and triblock copolymers comprising a poly(butyl acrylate) (PBA) first or middle block, and poly(methyl methacrylate) (PMMA) second or outer blocks, denoted MBA and MBAM, respectively, are prepared by nitroxide-mediated polymerization (NMP). Their particularity is that the acrylic block is controlled while the methacrylate block is polymerized via an uncontrolled radical process under the synthesis conditions used. Overall composition and molecular weight polydispersities are large. Molecular disorder does not yield macrophase separation, and TEM on solvent cast films reveals lamellar and poorly ordered bicontinuous, cylindrical, or spherical morphologies. Except for the lamellar phase, clear multiple orders of diffraction are not visible in SAXS, and scattering profiles instead indicate a liquidlike order of microdomains. More importantly, morphology boundaries are strongly shifted compared to those commonly accepted for model monodisperse block copolymers. Hence, symmetric copolymers adopt morphologies with highly curved interfaces while lamellae are displaced to PMMA-rich compositions. These results suggest that unbalanced polydispersity between the two blocks can induce interfacial curvature toward to broadest molecular weight distribution, thereby releasing stretching energy of the whole chain. This effect is expected to be encountered in radical or hybrid block copolymer syntheses whenever control cannot be optimized for all blocks.

I. Introduction

Microphase-separated block copolymers comprising two or more incompatible polymer blocks present great interest since they combine at the nanometer scale the intrinsic properties of different homopolymers. Highly ordered periodic lamellar, bicontinuous, cylindrical, or spherical nanostructures are typically observed. Multiblock or graft architectures, as in ABA triblock copolymers, further bring unique rubber elasticity[1] or toughness[2] arising from molecular bridges between different microdomains. Some of these advantages can also be harnessed in blends with homopolymers, provided macroscopic phase separation between copolymer-rich and homopolymer-rich domains can be avoided or limited during melt processing.[3,4]

For a model AB diblock with strong enough degree of segregation χN, where χ is the Flory−Huggins segmental interaction parameter and N the total number of segments in the copolymer chain, a lamellar phase is expected when both blocks occupy equal volume fractions, ϕ_i, and morphologies with curved interfaces—hexagonally packed cylinders and then closed-packed spheres—for increasingly asymmetric compositions.[5,6] For slight asymmetries and over a certain temperature range, the bicontinuous double-gyroid phase can also be observed. Phase diagrams and morphology boundaries of AB diblocks are not necessarily symmetric around $\phi_A = 0.5$ because of conformational asymmetry,[7,8] which is a measure of packing and chain flexibility differences between the two blocks. This effect has been investigated theoretically and quantified experimentally for the most studied diblock copolymers, for which complete phase diagrams have been determined. For multiblock and graft copolymers, architecture is an extra parameter that affects interfacial curvature and copolymer morphologies.

The vast majority of block copolymers used today is based on styrene, butadiene, isoprene, and their derivatives and prepared by living anionic polymerization.[9] This method produces tailored block copolymers of controlled molecular weight and molecular weight distribution (MWD), chain-end functionalization, and architecture, through precise sequencing of two, three, or even more monomers.[10] It has met great commercial success with SIS (polystyrene-*b*-polyisoprene-*b*-polystyrene) and SBS (polystyrene-*b*-polybutadiene-*b*-polystyrene) triblock copolymers,[11] despite the stringent synthesis conditions required. More recently, anionic polymerization has been extended to other commercially important vinyl monomers, among which acrylates or methacrylates.[12−15] Clever solutions overcoming technical obstacles such as very low reacting temperatures for these copolymers are starting to emerge.[16]

A very attractive alternative for the direct synthesis of block copolymers which remain challenging for anionic polymerization is controlled radical polymerization (CRP). Considerable

* To whom correspondence should be addressed.
† Current address: ARKEMA, King of Prussia, PA 19406.
‡ Current address: COATEX, France.

10.1021/ma060541u CCC: $33.50
Published on Web 07/22/2006

efforts in synthetic chemistry over the past two decades have indeed allowed the establishment of "living" polymerization schemes in free radical systems, with three main mechanisms: nitroxide-mediated polymerization (NMP),[17−20] atom transfer radical polymerization (ATRP),[21−23] and reversible addition−fragmentation transfer (RAFT).[24,25] For the first two, a reversible end-capping reaction of free-radical chain ends is artificially introduced that competes with common propagation and termination reactions. Provided the equilibrium between active and "dormant" (end-capped) chain ends favors the latter, instantaneous concentration of radicals is low and chances of irreversible termination are slim. Second, if initiation is fast compared to chain growth, molecular weights are controlled and their distribution is narrower. Third, growing chains remain in their end-capped state at the end of polymerization and can serve to initiate polymerization of a second type of monomer. These developments enable the preparation of novel block copolymers of various architectures from virtually all kinds of vinyl monomers by free radical mechanisms in common mass, suspension, or even emulsion processes.[26]

Most synthetic efforts in CRP originally focused on controlling the living character of chain ends and restrain compositional and architectural polydispersities as much as possible. Several initiator and/or catalysts systems have been designed that enable the laboratory-scale-controlled, though often slow, synthesis of novel copolymers of low to intermediate molecular weights. Their polydispersity index (PDI), defined as the ratio of weight- to number-average molecular weight M_w/M_n, typically lies around 1.2−1.4, seldom below 1.1. Although no systematic study has been reported, self-assembly and morphologies observed for these copolymers seem to correlate with those reported for model block copolymers.[27−29] When CRP is performed under economically attractive or industrially viable conditions, however, it is likely that side reactions inherent to free radical mechanisms will increase, along with compositional and architectural polydispersities. In attempting to fully harness the benefits of these developments, a compromise has to be found for each monomer or combination of monomers between increased rapidity or facility of synthesis and the progressive loss of control it is associated with. Accounting for synthesis imperfections and molecular disorder in these block copolymers has thus become a real necessity.

The potential impact of polydispersity and chemical disorder on block copolymer phase behavior was recognized early on[30] and has been treated by a variety of theoretical approaches ranging from weak/strong segregation analytical treatments[30−33] to full self-consistent schemes relying on numerical calculations.[34−36] Polydispersity is typically incorporated in a continuous form using a monomodal Shulz distribution of chain length amenable to analytical or numerical studies. Over 20 years ago, weak segregation studies by Leibler and Benoit[30] predicted three main effects of strong polydispersity on block copolymers above the order/disorder or microphase separation transition:[5] composition fluctuations become stronger and shift to larger length scales compared to monodisperse analogues with equivalent M_n, and the mixing of chains of different compositions can induce macroscopic (infinite wavelength) concentration fluctuations that progressively mask finite wavelength ones. Likewise, polydispersity was later predicted to increase microdomain spacings in the ordered state[31−34] and decrease the critical degree of segregation $(\chi N_n)_c$ for microphase separation, increasing incompatibility compared to monodisperse copolymers of equivalent M_n.[31,32,34] It can also shift or deform stability regions of the various morphologies[32,34] and leads to partitioning of the blocks according to their length within microdomains.[34,35] Similar trends are predicted when polydispersity is approximated by combinations of two delta functions, simulating bidisperse mixtures of monodisperse copolymers.[37−40] Such modeling has accompanied a large body of experimental studies on bidisperse blends.

Indeed, for anionic synthesis producing only narrow MWD, experimental investigations of the influence of substantial polydipsersity on block copolymer self-assembly originally concentrated on mixtures of nearly monodisperse copolymers of different composition and/or molecular weight. Miscibility criteria, phase behavior, and segment distributions within self-assembled morphologies of bimodal[41−46] and, more recently, multimodal[47] distributions correlate quite well with theory predictions. They illustrate how blending different copolymers can be effectively used to control interfacial curvature and self-assembled morphologies via the cosurfactant effect.[38,39,45,46] Provided molecular weights and/or compositions are not too disparate, different copolymer chains self-assemble around a common interface, and blends are microphase-separated. As predicted by theory, microdomain dimensions and spacings are always higher than the monodisperse analogues of these copolymer blends. For increasingly disparate copolymers, however, bidisperse or multimodal blends become partially miscible, and macrophase separation occurs over a certain range of blend composition.[40,46,47] This raises the important question of whether macro- or microphase separation dominates in strongly segregated block copolymers with similarly broad yet continuous molecular weight distributions. Recent studies by Bendejacq et al. indicate that copolymer chain distributions with PDI's as high as 2 obtained by CRP self-assemble and order, at least for low M_n.[48] Lynd and Hillmyer similarly report microdomain formation and ordering for low-M_n diblock copolymers comprising a monodisperse poly(ethylene-*alt*-propylene) block and a poly(DL-lactide) block whose polydispersity can be tuned from ∼1 to 2.[49] No macrophase separation was observed in these systems either. The PLA block polydispersity was further shown to affect microdomain formation and to induce changes in interfacial curvature in weakly segregated and slightly asymmetric copolymers.

In this work, we investigate the self-assembling capability and morphologies of high molecular weight block copolymers prepared by NMP. Di- and triblock copolymers of poly(butyl acrylate) (PBA) and poly(methyl methacrylate) (PMMA), denoted MBA and MBAM, respectively, are prepared at the laboratory and micropilot scale by radical polymerization controlled with the nitroxide *N*-*tert*-butyl-*N*-(1-diethylphosphono-2,2-dimethylpropyl)-*N*-oxyl, denoted DEPN.[19,50] Similar copolymers are being commercialized under the trademark Nanostrength and are used for the toughening via nanostructuration of thermoset or thermoplastic matrices compatible with PMMA blocks.[3,51] The copolymers studied comprise a first PBA block controlled and terminated by the nitroxide. This block is then used to initiate polymerization of PMMA outer or second blocks which are not as well controlled under the synthesis conditions used.[52,53] Self-assembly and mesoscopic order in the resulting polydisperse copolymers are studied by transmission electron microscopy (TEM) and small-angle X-ray scattering (SAXS). While precise interdomain distances in microphase-separated morphologies could be extracted from SAXS, the degree of lattice order was not sufficient to identify morphologies and symmetries with this technique. Direct observations with TEM were thus essential to investigate self-assembly in these polydipserse block copolymers. To this end, two staining protocols

Scheme 1. DEPN-Based Initiators Used for NMP of Acrylic Copolymers: (a) Mono- and (b) Dialkoxyamine

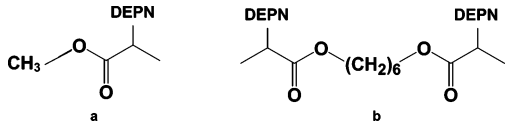

were developed that create TEM mass contrast between acrylic and methacrylic microdomains. The effect of polydispersity on observed bulk morphologies is discussed. Binary blends of these polydisperse copolymers are also presented.

II. Experimental Section

1. Block Copolymer Synthesis. Methyl methacrylate and *n*-butyl acrylate were purchased from Aldrich and used as received without any purification. DEPN and the DEPN-based alkoxyamine mono- and difunctional initiators (compounds **1** and **2**, Scheme 1) were prepared by ARKEMA as described previously[54,55] and used as is. Laboratory-scale bulk polymerizations were carried out under nitrogen in a glass reactor equipped with a stirring bar and a temperature probe. In a typical experiment, a mixture of butyl acrylate, alkoxyamine, and a 2.5 mol % excess free DEPN with respect to the alkoxyamine was degassed under a nitrogen flow for 20 min and then heated to 120 °C. Polymerization was allowed to proceed for a few hours to a conversion of ca. 50−70% to preserve the living character of polymer chains.[56] Residual BA monomer was stripped at 50 °C under vacuum ($p \sim 1 \times 10^{-3}$ bar). In a second step of the synthesis, MMA was added to the desired amount of dried BA−DEPN macroinitiators, degassed under nitrogen, and heated to 120 °C under 2.5 bar of pressure. Polymerization proceeded for 1−2 h and could only reach 40% conversion of MMA. This problem, known for DEPN-mediated polymerization of PMMA, has been attributed to a very high equilibrium constant between active and dormant species for this system. The resulting instantaneous concentration of propagating macroradicals is too large to gain control and strongly favors irreversible self-termination.[52,53] Yet, copolymers could be recovered after this second step and were purified by repeated dissolution in THF and precipitation in a mixture of methanol and water and then dried.

In some cases, statistic copolymers of butyl acrylate and styrene, denoted BAS, were prepared as first blocks by copolymerizing a mixture of BA with 30 wt % styrene. This copolymerization is also controlled and yields statistic copolymers at this composition.[57] Styrene monomers offer a straightforward and unambiguous way of staining soft acrylic microdomains and examine final copolymer morphologies by TEM. This, in turn, allowed us to confirm the validity of two novel staining protocols in the absence of styrene in these acrylic/methacrylic copolymers. Note that, based on simple group contribution calculations which have proven quite successful for styrene/acrylic/methacrylic systems,[58] replacing 30 wt % butyl acrylate monomers by styrene units in the first block should not strongly alter the segregation strength and phase behavior of the copolymers studied here. Indeed, a rough estimate of the respective Flory−Huggins interaction parameters can be obtained according to

$$\chi_{AB} = \frac{v}{RT}(\delta_A - \delta_B)^2 \quad (1)$$

where v is an average monomer volume, taken here as the geometric average $(v_A v_B)^{1/2}$, δ_A and δ_B are the solubility parameters of polymers A and B, respectively, R is the gas constant, and T is the absolute temperature. For an average monomer volume of 100 cm^3/mol, $\delta_{PMMA} = 19.65$ (J/cm^3)$^{1/2}$ and $\delta_{PBA} = 18.6$ (J/cm^3)$^{1/2}$ calculated as described previously[58] according to van Krevelen;[59] this yields an interaction parameter $\chi_{PMMA/PBA} = 0.03$ at 180 °C and 0.047 at room temperature, not incompatible with previous experimental studies on similar copolymers by Jérôme and co-workers.[60] Incorporating 30% styrene in the first block yields an effective interaction parameter between the PMMA block and the acrylic blocks calculated according to the well-known random copolymer effect:[61]

$$\chi_{eff} = (1 - f_S)\chi_{PMMA/BA} + f_S\chi_{PMMA/PS} - f_S(1 - f_S)\chi_{PBA/PS} \quad (2)$$

where f_S is the fraction of S units in the first block. With $\delta_{PS} = 18.2$ (J/cm^3)$^{1/2}$ and $v_{PS} = 98$ cm^3/mol,[58] this yields at 180 °C $\chi_{PBA/PS} = 0.007$, $\chi_{PMMA/PS} = 0.05$ (very close to the experimental value[62]), and $\chi_{eff} = 0.035$ for the MBAS block copolymers, i.e., very close to the $\chi_{PMMA/PBA}$ calculated above. Styrene units in the PBA blocks are thus expected to have a minor effect on phase behavior.

Larger scale syntheses of the block copolymers were also performed, this time in an industrial double-jacket stainless steel reactor of a capacity of 20 L and equipped with a pressure safety valve tarred at 5 bar. In this case, difunctional PBA macroinitiators, prepared as described above, did not contain any styrene. The PMMA blocks were polymerized in two steps to control the temperature rise. After 1 h at 105 °C, the reactor was heated to 120 °C for 30 min, after which reaction reached the limiting conversion of ca. 40 wt %. Block copolymers were recovered by stripping residual monomer at 190 °C under vacuum in a Clextral BC21 outgassing twin-screw extruder and then grinded.

Dilute solutions in THF of the macroinitiators and final copolymers were prepared for molecular weight and molecular weight distribution characterization by size exclusion chromatography (SEC). Composition was determined by ^{1}H NMR on dilute solutions in deuterated chloroform. The composition distribution of the final copolymers was measured by liquid adsorption chromatography (LAC).[63] This technique allows separation of copolymer chains according to their composition rather than molecular weight by using a solvent gradient whose polarity is judiciously varied over time. Note that this composition distribution complicates the absolute determination of average block copolymer molecular weights and PDI by SEC since the refractive index increment dn/dc, where n is the refractive index and c is the solution concentration, varies over the whole chain length distribution. The values given in Table 1 for block copolymers are thus only approximate, and further treatment to extract polydispersity of PMMA blocks was not attempted.

Table 1. Characteristics of PMMA/PBA Copolymers

copolymer[a]	PMMA (vol %)[b]	$10^{-3}M_n$ (g/mol)[c]	M_w/M_n	M_w/M_n PBA	$T_{g,soft}$ (°C)	$T_{g,hard}$ (°C)
MBAS88	87	101	1.8	1.3	−0.5	140
MBAS85	84	90	1.6	1.3	0.5	142
MBAS61	59	80	1.8	1.3	−3.5	110
MBAS60[d]	58	72	2.0	1.5	17.0	131
MBAS53	51	82	1.4	1.2	−2.6	134
MBAS49[d]	47	71	1.8	1.5	17.6	128
MBAM69	67	124	1.9	1.5	−38.0	129
MBAM50	48	80	2.4	1.9	−32.0	127
MBAM45	43	87	2.0	1.4	−35.0	125
MBAM37	35	61	1.7	1.5	−41.0	115

[a] The numbers in copolymer names refer to PMMA weight percents determined by ^{1}H NMR. [b] Based on mass densities at 25 °C of 1.06 and 1.15 g/cm^3 for PBA (or PBAS) and PMMA, respectively. [c] Based on a Mark−Houwink calibration for PBA. [d] These two copolymers contained 40 wt % S in the acrylic block, against 25−30 wt % for the others.

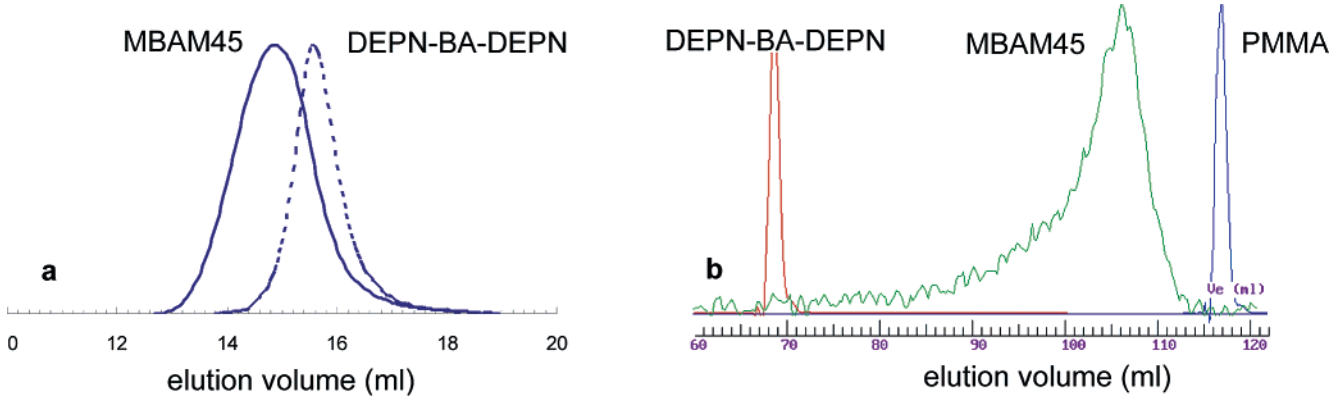

Figure 1. SEC (a) and LAC (b) traces of a PBA macroinitiator and related symmetric triblock copolymer MBAM45.

2. Block Copolymer Self-Assembly. Combined TEM and SAXS were used to investigate bulk self-assembled morphologies of the copolymers. Solvent cast films, ca. 700 μm thick, were obtained by slow evaporation over 2 weeks of 5 wt % solutions of the copolymers in toluene, followed by annealing under vacuum at 180 °C. For TEM observations, ultrathin sections, ca. 60 nm thick, were cut with a diamond knife from solvent cast films on a Leica Ultracut microtome. Microtoming was done at room temperature or under cryogenic conditions at −100 °C, depending on the BA fraction of the copolymers. Thin sections were collected on 400 mesh copper grids. When the PBA blocks contained styrene, sections were stained by ruthenium tetraoxide (RuO_4) vapor prior to TEM observations. Sample grids were held for 1−2 min above a 2 wt % aqueous solution of RuO_4. In a departure from previous reports on such copolymers, two staining protocols were also found to create TEM mass contrast between PMMA and PBA in the absence of styrene. The first one consists of liquid staining by completely immersing a pretrimmed sample block with a fresh surface in a 2 wt % RuO_4 aqueous solution for 24−48 h prior to sectioning. Diffusion of the liquid stain occurs over a few microns from the block surface and preferentially through the PBA elastomeric phase, which is physically stained. The sample block is then rinsed, dried, and placed in the microtome where sections among the first ones closest to the surface are collected on copper grids and ready for TEM observations. A second protocol, originally developed for staining semicrystalline polyamide,[64] was found to also work for preferential staining of PMMA over PBA. TEM copper grids with thin copolymer sections on the top were floated for 2 min at 60 °C onto a 2 wt % aqueous solution of phosphotungstic acid (H_3PO_4,-$12WO_3$, denoted PTA) and benzyl alcohol. Benzyl alcohol apparently acts as a dyeing assistant and helps PTA staining of PMMA. TEM micrographs were taken on sections prepared by these two methods and will be presented below. Micrographs were obtained on a JEOL 100CX microscope operated at an acceleration voltage of 100 kV and a Zeiss 902 microscope operated at 80 kV and equipped with a MegaviewII digital camera from Soft Imaging Systems.

The presence or absence of macrophase separation, the degree of long-range order, and main interdomain distances of these copolymers were also studied by SAXS at room temperature on the same solvent cast films. The Cu Kα radiation was used, and transmitted scattered intensity was collected on a linear detector LPS55 from INEL. The sample−detector distance was 1.9 m, resulting in a q range from 0.007 to 0.065 Å^{-1}. Scattered intensity was corrected for blank background scattering and is given in arbitrary units as a function of wave vector $q = (4\pi/\lambda) \sin \theta$, where θ is half the scattering angle and λ is the wavelength of 1.54 Å.

Microphase separation in these block copolymers comprising a soft PBA block and a hard PMMA one was also studied by dynamic mechanical analysis (DMA) on a DMA 2980 dynamic mechanical analyzer from TA Instruments. Rectangular bars, $L \times l = 20 \times 4$ mm, 0.3−0.8 mm thick, were placed in a sample holder operated in tension, and a small oscillatory tensile deformation with an amplitude of ∼0.2% was applied at a frequency of 1 Hz. Samples were cooled to −100 °C, and the evolution of storage (E') and loss (E'') Young moduli was recorded upon heating to 200 °C at 2 °C/min. T_g's of the microphases were taken at the maxima of tan δ given by the ratio of loss to storage modulus, where δ is the phase lag between the imposed oscillatory deformation and the dynamic response of the material.

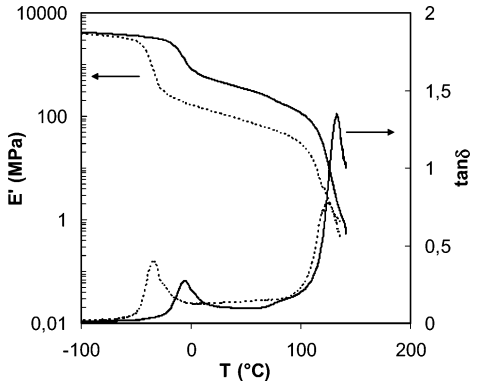

Figure 2. Evolution of E' and tan δ as a function of temperature for MBAM50 (dotted curves) and MBAS53 (full curves).

III. Results and Discussion

1. Neat Copolymers. Table 1 summarizes the characteristics of the acrylic MBAS*xx* diblock and MBAM*xx* triblock copolymers studied here, where *xx* refers to the weight percents of PMMA as determined by NMR. Their particularity is that the first acrylic block undergoes a living polymerization while the PMMA blocks are less controlled by the nitroxide used here. In all cases, monomodal molecular weight distributions were obtained, with polydispersities around 1.3−1.5 for the BA or BAS macroinitiators and around 2.0 for the final copolymers. This is illustrated by the SEC traces of Figure 1a for a symmetric MBAM triblock and the related PBA macroinitiator. As shown in Figure 1b, wide yet monomodal LAC signals of the final copolymers lay in between those of the PBA first block and PMMA standards. The breadth of the copolymer peak reflects composition polydispersity. In some cases, small traces of residual PBA or thermally initiated PMMA homopolymers, not visible by SEC, could also be detected by LAC. These small amounts of residual homopolymer were not extracted and are estimated to account for a few wt % at the most.

All copolymers investigated formed optically clear films and extruded strands, suggesting the absence of macrophase separation despite the broad composition and chain length distribution. DMA always indicated the presence of two microphases: one with a high T_g of ∼125 °C corresponding to PMMA and a soft microphase with a T_g ranging from −45 to −25 °C depending on the PBA block length. For copolymers with a PBAS first

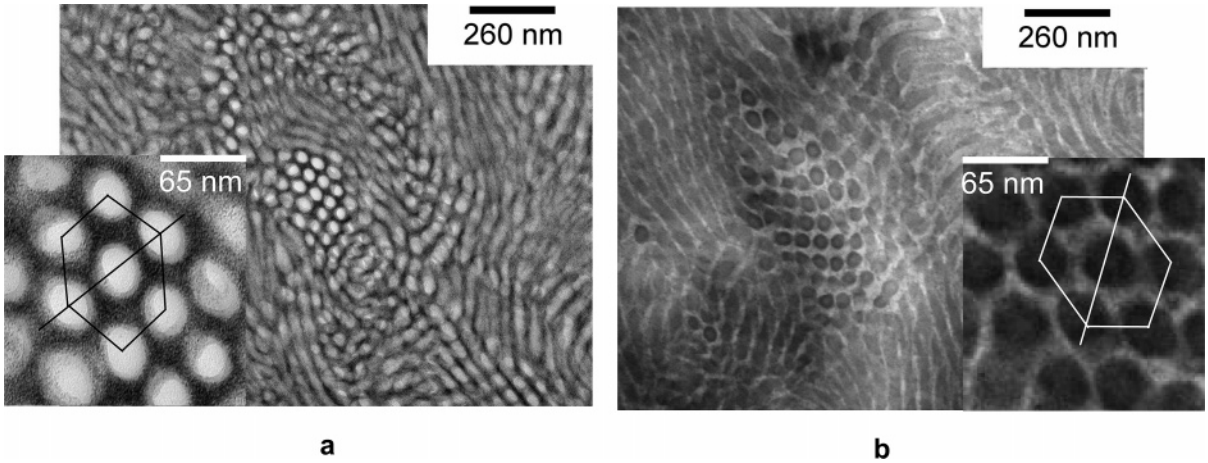

Figure 3. TEM micrographs of symmetric triblock copolymer MBAM50, solvent cast and annealed. (a) Liquid RuO_4 staining. PBA microdomains appear black while PMMA is white. (b) PTA/benzyl alcohol staining. PMMA microdomains are now black and PBA is white. Insets show local hexagonal packing.

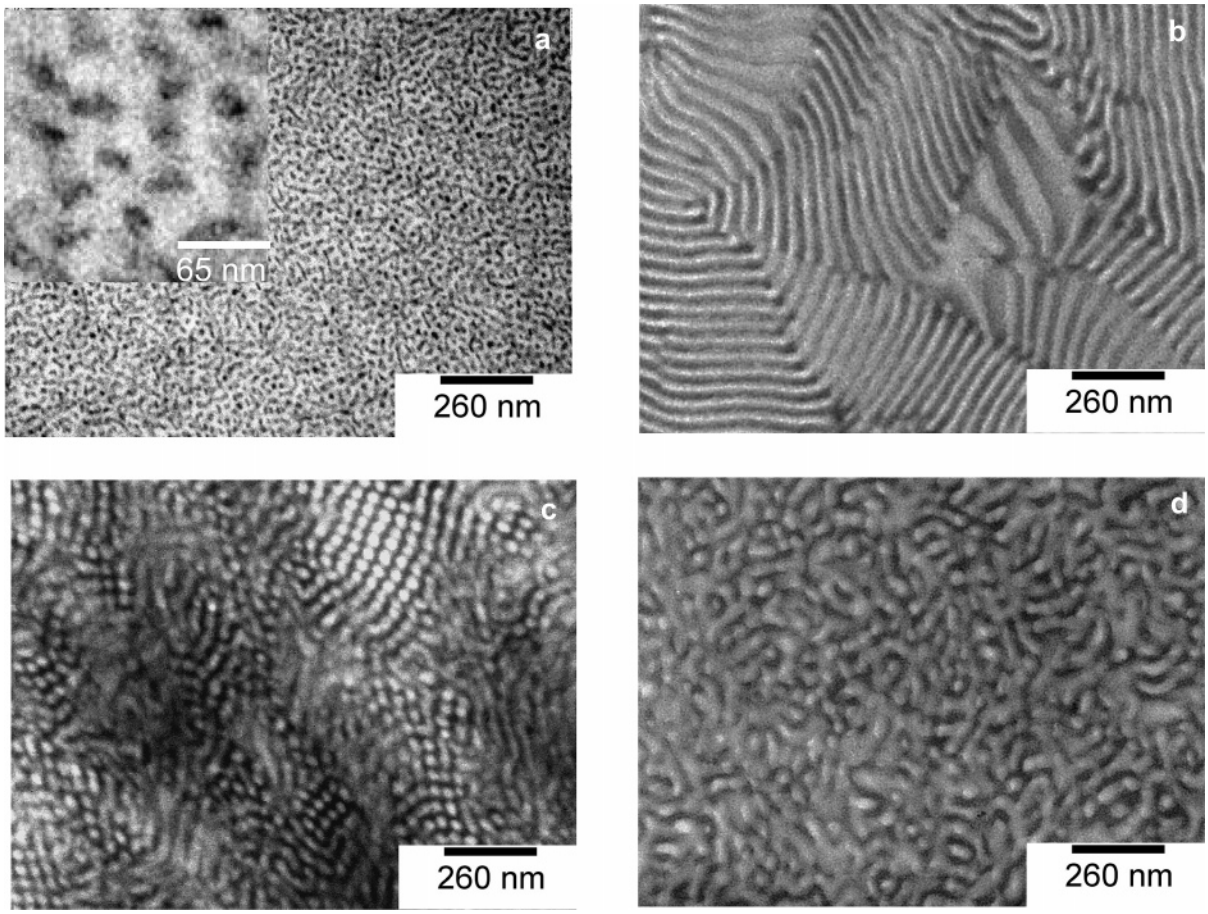

Figure 4. TEM micrographs for the series of MBAS diblock copolymers with compositions ranging from 87 to 47 vol % PMMA: (a) MBAS85, (b) MBAS60, (c) MBAS53, and (d) MBAS49. BAS blocks contain styrene units and were stained with RuO_4 vapor. They appear dark while PMMA microdomains are white.

block, the soft phase had a higher T_g of ~ -5 °C to 10 °C, sometimes higher but consistent with the amount of styrene incorporated in the first block. Figure 2 illustrates this with the evolution of E' and tan δ for two symmetric copolymers, the triblock MBAM50 and the diblock MBAS53. T_g's for these and all other copolymers were taken at the peak values of tan δ and are listed in Table 1.

TEM was used to investigate the morphologies of these microphase-separated materials, starting with the symmetric triblock MBAM50. Figure 3 gives micrographs obtained on thin sections of a solvent cast and annealed film of this copolymer, stained with two different methods. In the left micrograph, PBA microdomains were physically stained with liquid RuO_4 for 48 h and appear black while PMMA is white. In the right micrograph, PMMA was stained with a PTA/benzyl alcohol solution and appears black while PBA is white. These micrographs reveal a morphology consisting of short PMMA cylinders dispersed in a BA matrix. Hexagonal order is only very local, grains with a given cylinder orientation are small, and long-range order is poor. More importantly, the interface of this symmetric copolymer is clearly concave toward PMMA, a departure from the planar geometry expected for and indeed

Table 2. Morphologies and Interdomain Spacing of PMMA/PBA Copolymers

copolymer	morphology[a]	D_{SAXS} (nm)[b]	D_{TEM} (nm)[c]
MBAS88	S	35	30
MBAS85	S	38	40
MBAS61	L	58	55
MBAS60	L	52	50
MBAS53	C	59	55
MBAS49	C	57	50
MBAM69	L		45
MBAM50	C	55	50
MBAM45	C−S	51	50
MBAM37	S		30−40

[a] S stands for spherical micelles, L for lamellae, and C for cylinders with local hexagonal order or cylindrical micelles with no specific local order. [b] Interdomain spacing taken as $2\pi/q^*$. [c] Average spacing between micelles or planes of cylinders (for S or C) and lamellar period (for L) measured on TEM micrographs.

encountered in most symmetric and monodisperse linear block copolymers.[65] The latter adopt a lamellar morphology with junction points aligned along planar interfaces that reflect equivalent stretching of the copolymer blocks.[66] While the triblock architecture is expected to induce a slight lateral shift of the morphology boundaries,[67] it cannot explain the curved interface obtained here. In fact, the same effect is also observed for the symmetric MBAS diblock copolymers.

To further elucidate the effect of polydispersity on self-assembly in these copolymers, a series of diblocks listed in Table 1 were indeed prepared, with approximately constant M_n but with compositions ranging from 87 to 47 vol % PMMA. These diblocks contain 25−30 wt % S units incorporated in the acrylate block for simple RuO_4 vapor staining. Figure 4 illustrates the different types of morphologies observed by TEM and listed in Table 2 for this series of MBAS diblock copolymers. At high PMMA fractions (87 or 84 vol %), small PBA micelles finely dispersed in a matrix of PMMA are obtained, as shown in Figure 4a for MBAS85. Most micelles are spherical, though some elongated ones are also present. No long-range order but only a liquidlike order of spheres is present. The average micellar core radius measured on TEM micrographs is ∼10 nm, and the distance between micelles is about 40 nm. Decreasing the PMMA content to ∼60 vol % flattens the interface, and copolymers adopt a lamellar morphology, as illustrated in Figure 4b for MBAS60. The lamellar period D is about 55 nm. Grains are small, and multiple defects characteristic of lamellar phases are encountered. As suggested by the observations of Figure 3, the stability domain of the lamellar phase does not encompass symmetric compositions in these polydisperse copolymers. Around 50 vol %, the interface curves toward PMMA and short cylinders are obtained for MBAS53 (Figure 4c), similar to those observed for MBAM50. Again, grains are small, and hexagonal order is only very local. In hexagonal regions, the average distance between cylinders is ∼55 nm and the average cylinder radius is ∼15 nm. All observed symmetric copolymers adopted an interface curved toward PMMA, yet the aspect ratio of PMMA microdomains and the degree of order varied from sample to sample. Figure

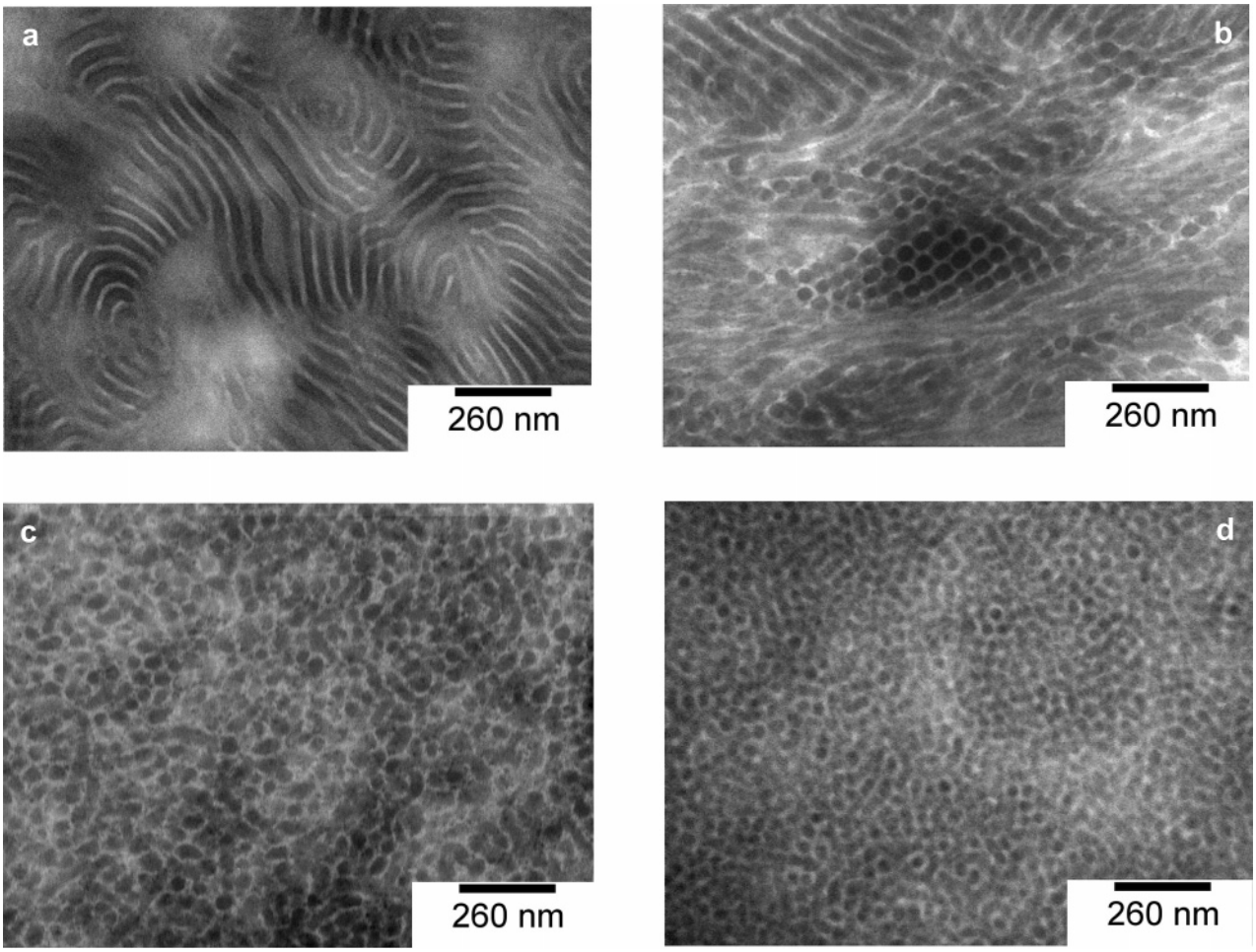

Figure 5. TEM micrographs of different MBAM triblock copolymers showing lamellae for MBAM69 (a), cylinders for MBAM50 (b), cylindrical or spherical micelles for MBAM45 (c), and spheres of PMMA for MBAM37 (d). PMMA microdomains are stained with a 2 wt % PTA/benzyl alcohol aqueous solution and appear black.

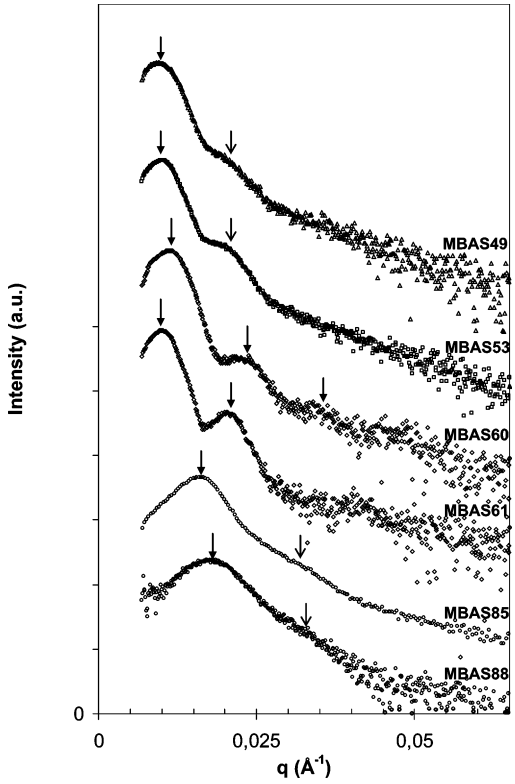

Figure 6. SAXS intensity profiles (arbitrary units, log scale) as a function of wave vector q for MBAS diblock copolymers listed in Table 1. Each profile has been shifted vertically for clarity. For lamellar copolymers (MBAS60 and MBAS61), little arrows indicate higher order Bragg reflections occurring at integer multiples of q^*, the main peak position. For all other copolymers, no clear higher order reflections can be identified, but more or less broad shoulders indicated by thinner arrows.

4d gives another example of cylindrical micelles in MBAS49, this time with no sign of hexagonal order but a continuous character. Once it curves around 50 vol %, the interface is expected to remain concave toward PMMA, and microdomains, cylindrical or spherical, should progressively decrease in size as the fraction of MMA decreases at constant molecular weight.

On the basis of the simple group contribution calculations presented above, the effect of styrene units in the PBA first block on self-assembly in these copolymers is expected to be minor. Entirely similar morphological trends were indeed also observed for all-acrylic MBAM triblock copolymers, with lamellae forming around 60 vol % PMMA (Figure 5a), cylinders or cylindrical micelles at symmetric compositions (Figure 5b,c), and spherical PMMA micelles at 35 vol % PMMA (Figure 5d).

Except for the lamellar phase, long-range order is always poor for these diblocks and triblocks. This is manifest in the SAXS profiles collected at room temperature on the same solvent cast films. Figure 6 gives transmitted scattered intensity profiles as a function of wave vector q for the series of MBAS diblock copolymers. At very high PMMA fractions, the profiles present a broad maximum indicated by a thick arrow at $q^* \sim 0.018$ Å^{-1} and $q^* \sim 0.017$ Å^{-1} for MBAS88 and MBAS85, respectively. Mild second-order shoulders around $2q^*$, more apparent for MBAS85, are consistent with the disordered spheres observed by TEM. Similar profiles have been obtained for monodisperse asymmetric block copolymers trapped in metastable transient states because of their slow dynamics[68] or heated above the lattice disordering transition, i.e., at high enough temperatures where microdomains are still present but only adopt a liquidlike order.[69−72]

Around 60 vol % PMMA, the copolymers adopt a lamellar morphology, and the SAXS profiles of Figure 6 present at least 2 orders of diffraction at multiple integers of $q^* \sim 0.01-0.012$. The lamellar period $D = 2\pi/q^*$ is reported in Table 2 and corresponds to that measured on TEM micrographs. The lamellar phase roughly extends from 65 to 55 vol % PMMA. At 50 vol %, the interface curves toward PMMA and a poorly ordered cylindrical morphology is observed by TEM (Figure 4c). SAXS profiles cannot be used to confirm this observation. No clear higher order reflections characteristic of hexagonal lattices can be identified, although the strong shoulder after the main peak located at $q^* \sim 0.01$ does not preclude an overlap of weak and broad $\sqrt{3}q^*$ and $\sqrt{4}q^*$ reflections. At 47 vol %, the shoulder is weaker and displaced to higher q values. This sample hardly presents any long-range order but just a liquidlike order of continuous cylindrical micelles (Figure 4d). Entirely similar profiles are obtained for the MBAM triblock copolymers, with clear higher order Bragg reflections only for lamellar compositions and shoulders indicating liquidlike order otherwise. Table 2 lists the average interdomain spacings extracted from SAXS profiles from the inverse of the scattering peak position ($2\pi/q^*$) as well as those measured on TEM micrographs for all the copolymers studied. The latter roughly correspond to SAXS measurements.

For lamellar copolymers, it is interesting to compare the experimentally observed lamellar period to that predicted for a hypothetical model monodisperse block copolymer of equivalent N_n. For monodisperse diblocks, strong segregation theory predicts that[66]

$$D = \frac{4}{\sqrt{6}}\left(\frac{3}{\pi^2}\right)^{1/3} a N^{2/3} \chi^{1/6} \qquad (3)$$

where a is the average statistical segment length. With a estimated to be 7 Å for PMMA/PBA,[73,74] the interaction parameter χ calculated at room temperature according to eq 1, and a rather high approximate value of N_n of 900, eq 2 yields a theoretical lamellar period of ~43 nm for a monodisperse hypothetical PMMA/PBA diblock. This is still lower than the SAXS values of 58 and 52 nm listed in Table 2 for the two polydisperse diblocks considered, consistent with the prediction[30−34] and experimental observation[47−49] that continuous polydispersity increases domain spacing compared to monodisperse copolymers of equivalent M_n. A similar effect has been reported for binary blends of two diblock copolymers. Zhulina and Birshtein[37] derived an analytical expression for D in these systems that captures this swelling induced by polydispersity and was successfully used by Court and Hashimoto to describe their experimental results.[45] A similar analytical expression for D is unfortunately not readily available for continuous polydispersity. Yet, our results seem to confirm that eq 2 with an appropriate M_n is not sufficient to describe lamellar spacing, which also depends on overall PDI.

Self-assembly in the polydisperse copolymers investigated here can thus be summarized as follows. First, polydispersity in these high molecular weight systems does not lead to macrophase separation, consistent with low molecular weight polydisperse copolymers[48] and in contrast with discrete distributions of M_n and composition.[47] Surprisingly, long-range order is very difficult to achieve and sometimes completely absent in these copolymers, even after prolonged annealing at high temperature. Sharp and multiple orders of diffraction are absent from the scattered profiles which, for the most part, indicate liquidlike order of microdomains. It is interesting to note that continuous polydispersity is predicted to induce trapped lattice

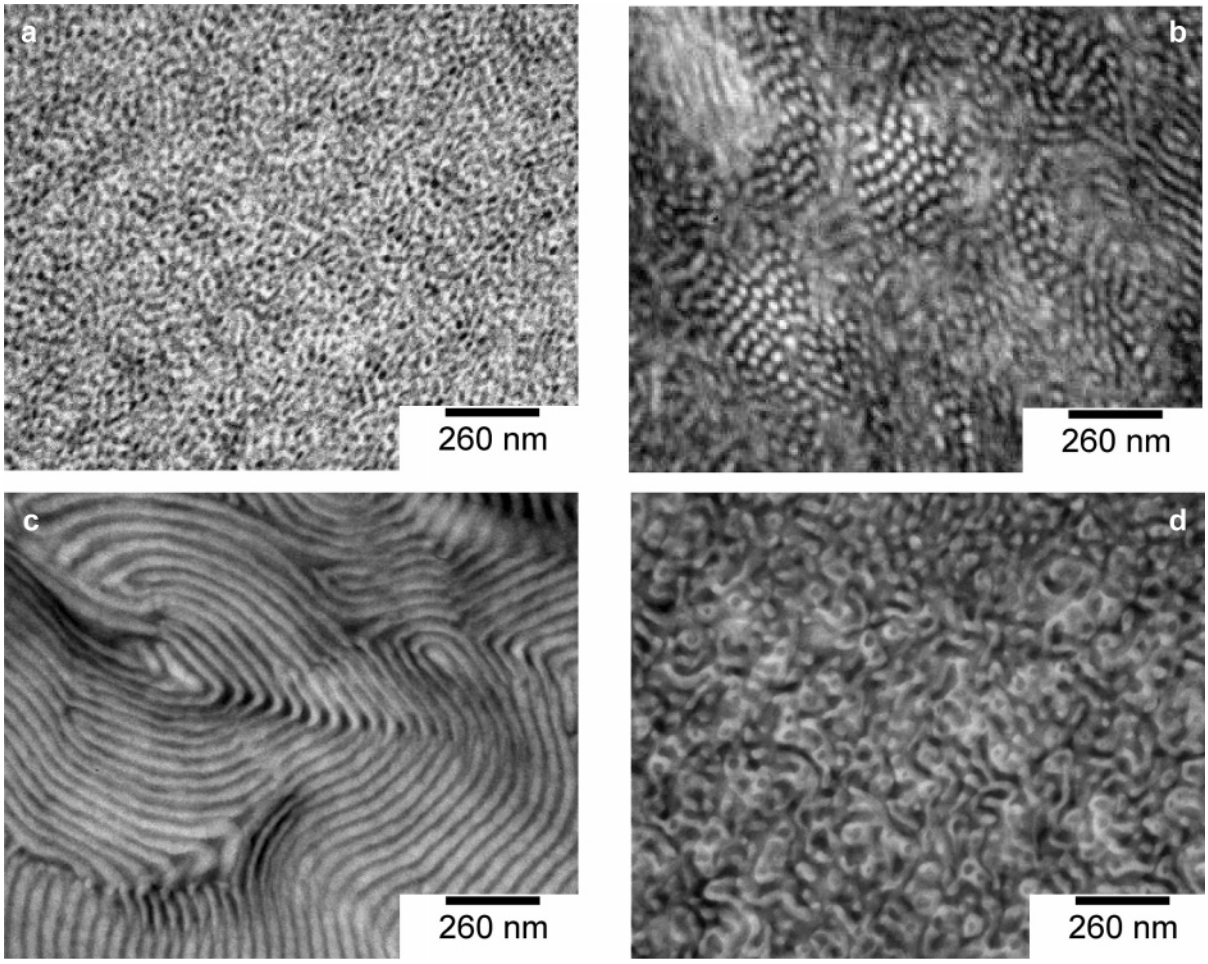

Figure 7. TEM micrographs of (a) MBAS85 and (b) MBAS53 and for two blends of these copolymers with global PMMA fractions of (c) 64 vol % PMMA (40/60 wt % blend of MBAS85/MBAS53) and (d) 72 vol % PMMA (66/44 wt % blend). BAS blocks are stained with RuO_4 vapor and appear black while PMMA is white.

disordering and defects in block copolymers.[34] These may take a long time to anneal, especially for the high molecular weights used here. In the future, we will test whether shear orientation can be used to increase lattice ordering in these copolymers.

But most importantly, disproportionate polydispersity between the two blocks appears to induce interfacial curvature toward the broadest molecular weight distribution and a resulting lateral shift of morphology boundaries. Indeed, cylinders or even spheres of PMMA are already stable at symmetric compositions. While conformational asymmetry may partly explain this observation, the magnitude of this effect is usually weaker.[7,8] Moreover, for the PMMA/PBA pair, the estimation of $\epsilon = (a_A^2/v_A)/(a_B^2/v_B)$, the parameter commonly used to quantify conformational asymmetry between A and B, where a_i and v_i are the statistical segment length and monomer volume of polymer i, respectively, does not support this. Taking mass densities at 180 °C for PMMA and PBA of 1.10 and 0.93 g/cm^3, respectively,[75] a statistical segment length of 6.5 Å for PMMA and of 7.4 Å for PBA[73,74] yields $\epsilon \sim 1.17$ (here, A is PMMA and B is PBA). This is less than PS−PI diblock copolymers, for which the effect of conformational asymmetry is modest compared to the shifts observed here. Even if we had over- or underestimated a_{PBA} which is not precisely known, conformational asymmetry is not likely to be determinant for this system and apparently cannot explain the formation of cylinders at symmetric copolymer compositions. This observation is more likely related to the asymmetry in block polydispersity. In fact, it is not without reminding the well-known cosurfactant effect observed in binary blends of monodisperse copolymers. Interfacial curvature can be induced in the latter for mixtures of two AB diblocks with identical A blocks but short and long B blocks.[45,46] More recent theoretical predictions incorporating a continuous molecular weight distribution for the B blocks of an AB diblock lead to similar conclusions.[34] These calculations are directly related to the practical situation of uneven control between the different blocks of a copolymer encountered here. They predict that model AB copolymers forming hexagonally packed cylinders of B evolve into a spherical morphology when polydispersity of the B blocks is increased from 1 to 1.5 while A blocks remain monodisperse. Experiments on low mass model copolymers with one block displaying tunable polydispersity seem to confirm this prediction,[49] with the evolution of the double gyroid into a cylindrical morphology as the minority block polydispersity is increased from 1.37 to 1.43. Interestingly, symmetric copolymers considered in this study always remained lamellar, no matter how high the polydispersity of the second block, and induced interfacial curvature was only reported for weakly segregated and slightly asymmetric copolymers. This is in contrast with the present polydipserse copolymers for which cylinders or cylindrical micelles with highly curved interfaces form at symmetric compositions while lamellae are displaced to the composition range around 60 vol % PMMA. Note that dynamic rheological testing performed on some of the lamellar di- or triblock copolymers (data not shown) indicates microphase separation up to 220 °C, the highest measurement temperature. This is consistent with calculated values of χN_n at 180 °C lying

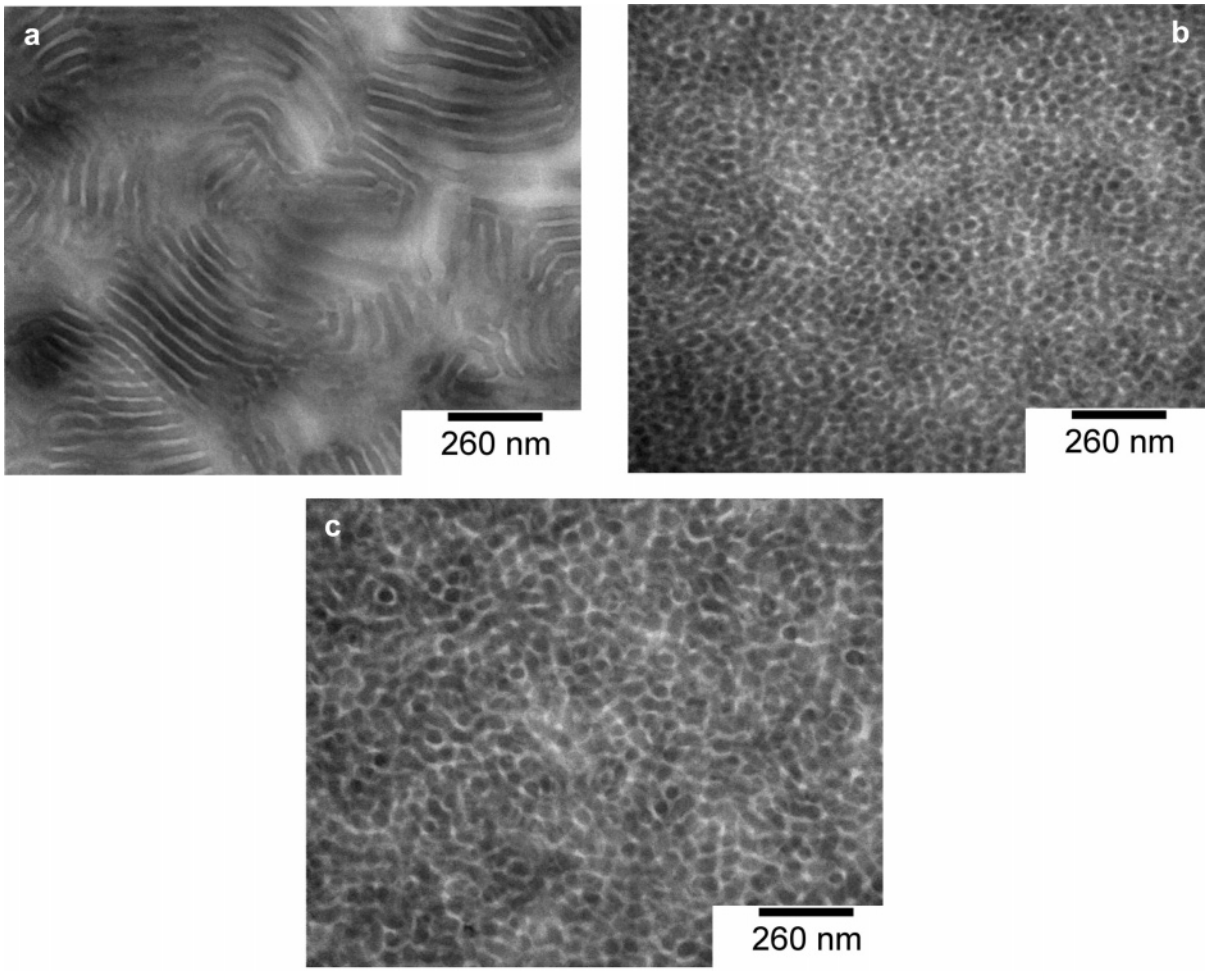

Figure 8. TEM micrographs of (a) MBAM69, (b) MBAM37, and (c) a blend of these two copolymers with a global PMMA fraction of 48 vol % PMMA (40/60 wt % blend of MBAM69/MBAM37). PMMA microdomains are stained with a 2 wt % PTA/benzyl alcohol aqueous solution and appear black while PBA microdomains are white.

between 20 and 30, which should be well into the ordered state since polydispersity shifts phase boundaries to lower χN_n values. These copolymers are thus not expected to be in the vicinity of the MST, even at the annealing temperature.

The presumed influence of unbalanced polydispersity between the two blocks on interfacial curvature and the resulting morphology shifts observed here can be qualitatively understood as follows. A first effect is the progressive dissolution of the shortest PMMA blocks into the PBA microdomains, especially at intermediate to low fractions of PMMA. Theoretical modeling of similar polydisperse copolymers indeed predicts that, for asymmetric compositions, some of the shortest polydisperse blocks dissolve into the matrix composed of monodisperse blocks.[34] Second, unbalanced stretching on both sides of the copolymer interface due to the higher polydispersity of PMMA blocks might induce interfacial curvature even at symmetric compositions. This is the cosurfactant effect: short and intermediate chains decorate the interface while the longest ones swell microdomains. Such segregation of chains according to their length within microdomains is indeed also predicted by theory. Here, it seems to results in a lateral compression of morphology boundaries toward PMMA-rich compositions.

2. Binary Blends of Polydisperse Copolymers. The robustness of morphological trends in the polydisperse copolymers studied here prompted us to further test their behavior in binary blends. To this end, two copolymers with opposite mean interfacial curvature, namely MBAS85 and MBAS53, were dissolved in toluene, and solutions were allowed to evaporate slowly over ~2 weeks. Two blends containing 66 and 40 wt % MBAS85, yielding overall volume fractions of PMMA of 72 and 64 vol %, respectively, were prepared. The resulting optically clear films were annealed at 180 °C for 2 days under vacuum. TEM and SAXS (not shown) reveal the absence of macrophase separation into two distinct regions rich in one or the other type of copolymer in these binary blends. Microphase-separated morphologies are shown in Figure 7 and compared to the neat copolymer morphologies. They appear to fit with the overall PMMA fraction of the blends: at 64 vol % PMMA, the blend of antisymmetric copolymers forms lamellae (Figure 7c), while at 72 vol % PMMA, a cocontinuous morphology that resembles polymeric microemulsions[76] is obtained (Figure 7d). These results strongly resemble those obtained on model binary blends of monodisperse copolymers of equal molecular weights but antisymmetric compositions.[41] Here, two copolymers with convex and concave interfaces mix intimately, and junction points align along a single interface which is planar for an overall PMMA fraction of 64 vol % and cocontinuous at 75 vol % PMMA. SAXS profiles, not shown here, confirm the lamellar phase of the 64 vol % blend, with two clear scattering peaks at q^* and $2q^*$. The SAXS lamellar period of 47 nm corresponds to the rough estimate of 40 nm obtained from TEM.

The blends described above are characterized by broad molecular weight and composition distributions and still self-assemble. It is interesting to further probe the stability of such polydisperse blends when average molecular weights of the constituting copolymers are no longer comparable. In binary

blends of monodisperse copolymers with antisymmetric compositions, macrophase separation has been observed for molecular weight ratios of the two copolymers as low as 2, while higher ratios of 5−10 are tolerated when compositions are close. Here, polydispersity may help prevent macrophase separation. Mixtures of MBAM69 and MBAM37 triblocks are good candidates to test this. Both copolymers were made out of the same PBA block, but the former has long PMMA outer blocks and a large overall M_n of 124 kg/mol, while the latter has short PMMA outer blocks and a much lower M_n of 61 kg/mol. A blend containing 40 wt % of MBAM69, with an overall PMMA fraction of 48 vol %, was prepared as described above, and the morphology observed by TEM is shown in Figure 8 and compared to those of the neat copolymers. The blend is transparent and single-phased and adopts a micellar morphology with strong interfacial curvature toward PMMA blocks. Most micelles appear to be spherical and have an average diameter of 35 nm and an average interdomain spacing of 55 nm. These results are entirely consistent with the morphological trends presented in section III.1. They further illustrate the robustness of self-assembly despite substantial molecular disorder in these copolymers.

IV. Conclusions

High molecular weight polydisperse acrylic block copolymers prepared by NMP were shown to self-assemble into various nanostructures despite substantial molecular disorder. Macrophase separation was never observed in any of the systems investigated. The morphologies of solvent cast and annealed copolymer films present little long-range order, and grains of a given microdomain orientation are small. The resulting SAXS profiles seldom display multiple orders of reflection, except for the lamellar phase. For all other morphologies with curved interfaces, SAXS profiles only indicate liquidlike ordering of microdomains with a main scattering peak followed by a broad shoulder around $2q^*$. More importantly, interfacial curvature does not follow the classical evolution with composition observed for ideal monodisperse block copolymers. Hence, lamellae are observed around 65−55 vol % PMMA, while perfectly symmetric copolymers adopt a curved interface concave toward PMMA and form cylinders or cylindrical micelles with poor lattice order. This is unlikely a result of conformational asymmetry. It was rather attributed to unbalanced polydispersity between the two blocks arising from the lack of control over polymerization of PMMA under the synthesis conditions used. Lower stretching of the more polydisperse PMMA brush apparently induces interfacial curvature and an overall lateral shift of the phase diagram toward compositions rich in PMMA. This cosurfactant effect might be expected in many systems prepared by controlled radical polymerization, though its magnitude may not be as dramatic as reported here. Blends of two polydisperse copolymers with opposite interfacial curvature but similar M_n were also prepared. The resulting systems are characterized by broad molecular weight distributions for both blocks and still self-assemble. Lamellae and a bicontinuous morphology were observed at overall PMMA fractions of 64 and 75 vol %, respectively. Mixing two triblock copolymers made out of the same PBA block but with large and short PMMA blocks, respectively, also yields a self-assembled blend which follows the trends observed for the neat triblocks. This is despite the even broader molecular weight distribution for PMMA. These results confirm the robustness of self-assembly of these polydisperse copolymers.

The morphological trends summarized above were observed under static conditions as close as possible to thermodynamic equilibrium. In practice, however, such copolymers are more likely to be used directly after processing from the melt in extruders and injection molders or in blends with homopolymers. This raises an important question regarding the effect of complex flow fields in polymer processing tools on self-assembly of these polydisperse systems and the related impact on end-use properties.

Acknowledgment. We thank C. Degoulet and M. Millequant for SEC and LAC analyses and B. Pouchan-Lahorre and P. Coupard for their help and precious advice on TEM. We are deeply indebted to P. Tordo, B. Charleux, and M. Cloitre for helpful discussions. This work was supported by CNRS, ESPCI, and ARKEMA. A.-V. Ruzette also acknowledges partial financial support from the Chateaubriand Fellowship and the European Commission.

References and Notes

(1) Holden, G.; Legge, N. R.; Quirk, R.; Schroeder, H. E. *Thermoplastic Elastomers*; Hanser: Munich, Germany, 1996.
(2) Ryu, C. Y.; Ruokolainen, J.; Fredrickson, G. H.; Kramer, E. J.; Hahn, S. F. *Macromolecules* **2002**, *35*, 2157.
(3) Ruzette, A. V.; Leibler, L. *Nat. Mater.* **2005**, *4*, 19.
(4) Leibler, L. *Prog. Polym. Sci.* **2005**, *30*, 898.
(5) Leibler, L. *Macromolecules* **1980**, *13*, 1602.
(6) Helfand, E.; Wasserman, Z. R. In *Developments on Block Copolymers*; Goodman, I., Ed.; Elsevier: New York, 1982; Vol. 1.
(7) Vavasour, J. D.; Whitmore, M. D. *Macromolecules* **1993**, *26*, 7070.
(8) Bates, F.; Schulz, M. F.; Khandpur, A. K.; Förster, S.; Rosedale, J. H.; Almdal, K.; Mortensen, K. *Faraday Discuss.* **1994**, *98*, 7.
(9) Szwarc, M. *J. Polym. Sci., Part A: Polym. Chem.* **1998**, *36*, 9.
(10) Hadjichristidis, N.; Pispas, S.; Floudas, G. *Block Copolymers: Synthetic Strategies, Physical Properties, and Applications;* John Wiley & Sons: New York, 2003.
(11) Holden, G.; Milkovich, R. U.S. Patent, 3,265,765, 1966.
(12) Riess, G.; Schlienger, M.; Marti, S. *J. Macromol. Sci. Phys.* **1980**, *B17*, 355.
(13) Stadler, R.; Auschra, C.; Beckmann, J.; Krappe, U.; Voigt-Martin, I.; Leibler, L. *Macromolecules* **1995**, *28*, 3080.
(14) Hong, K. L.; Uhrig, D.; Mays, J. W. *Curr. Opin. Solid State Mater. Sci.* **1999**, *4*, 531.
(15) Jérôme, R.; Teyssié, P.; Vuillemin, B.; Zundel, T.; Zune, C. *J. Polym. Sci., Part A: Polym. Chem.* **1999**, *37*, 1.
(16) Navarro, C.; Marcarian, X.; Vuillemin, B. *Macromol. Symp.* **1998**, *132*, 263.
(17) Moad, G.; Rizzardo, E.; Solomon, D. H. *Macromolecules* **1982**, *15*, 909.
(18) Listigovers, N. A.; Georges, M. K.; Odell, P. G.; Keoshkerian, B. *Macromolecules* **1996**, *29*, 8992.
(19) Grimaldi, S.; Finet, J.-P.; Le Moigne, F.; Zeghdaoui, A.; Tordo, P.; Benoit, D.; Fontanille, M.; Gnanou, Y. *Macromolecules* **2000**, *33*, 1141.
(20) Hawker, C. J.; Bosman, A. W.; Harth, E. *Chem. Rev.* **2001**, *101*, 3661.
(21) Wang, J.-S.; Matyjaszewski, K. *J. Am. Chem. Soc.* **1995**, *117*, 5614.
(22) Kato, M.; Kamigaito, M.; Sawamoto, M.; Higashimura, T. *Macromolecules* **1995**, *28*, 1721.
(23) Matyjaszewski, K. *Macromol. Symp.* **2001**, *174*, 51.
(24) Chiefari, J.; Chong, Y. K.; Ercole, F.; Krstina, J.; Jeffery, J.; Le, T. P. T.; Mayadunne, R. T. A.; Meijs, G. F.; Moad, C. L.; Moad, G.; Rizzardo, E.; Thang, S. H. *Macromolecules* **1998**, *31*, 5559.
(25) Moad, G.; Mayadunne, R. T. A.; Rizzardo, E.; Skidmore, M.; Thang, S. H. *Macromol. Symp.* **2003**, *192*, 1.
(26) Nicolas, J.; Charleux, B.; Guerret, O.; Magnet, S. *Macromolecules* **2004**, *37*, 4453.
(27) Leclère, P.; Moineau, G.; Minet, M.; Dubois, P.; Jérôme, R.; Brédas, J. L., Lazzaroni, R. *Langmuir* **1999**, *15*, 3915.
(28) Tong, J. D.; Moineau, G.; Leclère, P.; Brédas, J. L.; Lazzaroni, R., Jérôme, R. *Macromolecules* **2000**, *33*, 470.
(29) Matyjaszewski, K. *Prog. Polym. Sci.* **2005**, *30*, 858.
(30) Leibler, L.; Benoit, H. *Polymer* **1981**, *22*, 195.
(31) Hong, K. M.; Noolandi, J. *Polym. Commun.* **1984**, *25*, 265.
(32) Burger, C.; Ruland, W.; Semenov, A. N. *Macromolecules* **1990**, *23*, 3339.
(33) Milner, S. T.; Witten, T. A.; Cates, M. E. *Macromolecules* **1989**, *22*, 853.
(34) Sides, S. T.; Fredrickson, G. H. *J. Chem. Phys.* **2004**, *121*, 4974.
(35) Jiang, Y.; Chen, T.; Ye, F. W.; Liang, H. J.; Shi, A.-C. *Macromolecules* **2005**, *38*, 6710.

(36) Fredrickson, G. H. *The Equilibrium Theory of Inhomogeneous Polymers*; Oxford University Press: Oxford, UK, 2005.
(37) Birshtein, T. M.; Liatskaya, Y. V.; Zhulina, E. B. *Polymer* **1990**, *31*, 2185. Zhulina, E. B.; Birshtein, T. M. *Polymer* **1991**, *32*, 1299. Birshtein, T. M.; Liatskaya, Y. V.; Zhulina, E. B. *Polymer* **1992**, *33*, 332, 343, 2750.
(38) Shi, A.-C.; Noolandi, J. *Macromolecules* **1994**, *27*, 2936. Shi, A.-C.; Noolandi, J.; Hoffmann, H. *Macromolecules* **1994**, *27*, 6661.
(39) Spontak, R. J. *Macromolecules* **1994**, *27*, 6363.
(40) Matsen, M. W.; Bates, F. S. *Macromolecules* **1995**, *28*, 7298. Matsen, M. W. *J. Chem. Phys.* **1995**, *103*, 3268.
(41) Hashimoto, T.; Yamasaki, K.; Koizumi, S.; Hasegawa, H. *Macromolecules* **1993**, *26*, 2895. Hashimoto, T.; Koizumi, S.; Hasegawa, H. *Macromolecules* **1994**, *27*, 1562.
(42) Mayes, A. M.; Russell, T. P.; Deline, V. R.; Satija, S. K.; Majkrzak, C. F. *Macromolecules* **1994**, *27*, 7447.
(43) Vilesov, A. D.; Floudas, G.; Pakula, T.; Melenevskaya, E. Y.; Birshtein, T. M.; Lyatskaya, Y. V. *Macromol. Chem. Phys.* **1994**, *195*, 2317.
(44) Koneripalli, N.; Levicky, R.; Bates, F. S.; Matsen, M. W.; Satija, S. K.; Ankner, J.; Kaiser, H. *Macromolecules* **1998**, *31*, 3498.
(45) Court, F.; Hashimoto, T. *Macromolecules* **2001**, *34*, 2536. Court, F.; Hashimoto, T. *Macromolecules* **2002**, *35*, 2566.
(46) Hashimoto, T.; Yamaguchi, D.; Court, F. *Macromol. Symp.* **2003**, *195*, 191. Yamaguchi, D.; Hashimoto, T. *Macromolecules* **2001**, *34*, 6495 and references therein.
(47) Matsushita, Y.; Noro, A.; Iinuma, M.; Suzuki, J.; Ohtani, H.; Takano, A. *Macromolecules* **2003**, *36*, 8074. Noro, A.; Iinuma, M.; Suzuki, J.; Takano, A.; Matsushita, Y. *Macromolecules* **2004**, *37*, 3804. Noro, A.; Cho, D.; Takano, A.; Matsushita, Y. *Macromolecules* **2005**, *38*, 4371.
(48) Bendejacq, D.; Ponsinet, V.; Joanicot, M.; Loo, Y.-L.; Register, R. A. *Macromolecules* **2002**, *35*, 6645.
(49) Lynd, A. N.; Hillmyer, A. M. *Macromolecules* **2005**, *38*, 8803.
(50) Benoit, D.; Grimaldi, S.; Robin, S.; Finet, J. P.; Tordo, P.; Gnanou, Y. *J. Am. Chem. Soc.* **2000**, *122*, 5929.
(51) Ruzette, A.-V.; Chauvin, F.; Guerret, O.; Bertin, D.; Vuillemin, B.; Leibler, L.; Gérard, P. FR 02.00814.
(52) Ananchenko, G. S.; Souaille, M.; Fischer, H.; Le Mercier, C.; Tordo, P. *J. Polym. Sci., Part A: Polym. Chem.* **2002**, *40*, 3264.
(53) Charleux, B.; Nicolas, J.; Guerret, O. *Macromolecules* **2005**, *38*, 5485.
(54) Couturier, J. L.; Guerret, O.; Bertin, D.; Gigmes, D.; Marque, S.; Tordo, P.; Chauvin, F.; Dufils, P. E. WO 2004/014926.
(55) Guerret, O.; Couturier, J.-L.; Vuillemin, B.; Lutz, J. F.; Le Mercier, C.; Robin, S. Fr. Patent FR99.06329.
(56) Chauvin, F. Acrylic nanostructured materials by controlled radical synthesis. Ph.D. Thesis, University of Provence, Aix-Marseille I, 2002.
(57) Mignard, E.; Leblanc, T.; Bertin, D.; Guerret, O.; Reed, W. F *Macromolecules* **2004**, *37*, 966.
(58) Ruzette, A.-V. G.; Banerjee, P.; Mayes, A. M.; Pollard, M.; Russell, T. P.; Jerome, R.; Slawecki, T.; Hjelm, R.; Thiyagarajan, P. *Macromolecules* **1998**, *31*, 8509. Ruzette, A.-V. G. Molecular Design of Ordering Transitions in Block Copolymers. Ph.D. Thesis, MIT, 2000.
(59) Van Krevelen, D. W.; Hoftyzer, P. J. *Properties of Polymers. Correlations with Chemical Structure*; Elsevier: New York, 1972.
(60) In ref 28, Jerôme and co-workers estimate the ODT of a monodisperse 66 kg/mol MBAM triblock containing 24 wt % PMMA to lie around 155 °C. This would yield a $\chi_{PMMA/PBA} \sim 0.06$.
(61) Kambour, R. P.; Bendler, J. N.; Bopp, R. C. *Macromolecules* **1983**, *16*, 753.
(62) Stühn, B. *J. Polym. Sci., Part B: Polym. Phys.* **1992**, *30*, 1013.
(63) Degoulet, C.; Perrinaud, R.; Ajdari, A.; Prost, J.; Benoit, H.; Bourrel, M. *Macromolecules* **2001**, *34*, 2667.
(64) Corté, L.; Beaume, F.; Leibler, L. *Polymer* **2005**, *46*, 2748.
(65) See Hamley, I. W. *The Physics of Block Copolymers*; Oxford University Press: Oxford, 1998, and references therein.
(66) Semenov, A. N. *Sov. Phys. JETP* **1985**, *61*, 733.
(67) Mayes, A. M.; Olvera de la Cruz, M. *J. Chem. Phys.* **1989**, *91*, 7228; *J. Chem. Phys.* **1991**, *95*, 4670.
(68) Chu, J. H.; Rangarajan, P.; Adams, J. L.; Register, R. A. *Polymer* **1995**, *36*, 1569.
(69) Kinning, D. J.; Thomas, E. L. *Macromolecules* **1984**, *17*, 1712.
(70) Sota, N.; Sakamoto, N.; Saijo, K.; Hashimoto, T. *Macromolecules* **2003**, *36*, 4534.
(71) Kim, J. K.; Lee, H. H.; Sakurai, S.; Aida, S.; Masamoto, J.; Nomura, S.; Kitagawa, Y.; Suda, Y. *Macromolecules* **1999**, *32*, 6707.
(72) Abuzaina, F. M.; Patel, A. J.; Mochrie, S.; Narayanan, S.; Sandy, A.; Garetz, B. A.; Balsara, N. P. *Macromolecules* **2005**, *38*, 7090.
(73) Fetters, L. J.; Lohse, D. J.; Graessley, W. W. *J. Polym. Sci., Part B: Polym. Phys.* **1999**, *37*, 1023.
(74) While the value of a_{PMMA} is known to be about 6.5−6.7 Å, that of PBA is not directly known. Data from ref 73 on several acrylates, however, suggest a realistic value of a_{PBA} of 7.4 Å, yielding an average segment size of ∼7 Å, good enough to calculate an approximative lamellar period.
(75) Zoller, P.; Walsh, D. J. *Standard Pressure−Volume−Temperature Data for Polymers*; Technomic Publishing: Lancaster, PA, 1995.
(76) Bates, F. S.; Maurer, W. W.; Lipic, P. M.; Hillmyer, M. A.; Almdal, K.; Mortensen, K.; Fredrickson, G. H.; Lodge, T. P. *Phys. Rev. Lett.* **1997**, *79*, 849.

MA060541U